

SPATIAL OFFSETS IN FLARE-CME CURRENT SHEETS

JOHN C. RAYMOND,

Harvard-Smithsonian Center for Astrophysics, 60 Garden St., Cambridge, MA 02138, USA

SILVIO GIORDANO

INAF-Osservatorio Astrofisico di Torino, via Osservatorio 20, I-10025 Pino Torinese, Italy

AND

ANGELA CIARAVELLA

INAF-Osservatorio Astronomico di Palermo, P.za Parlamento 1, I-90134 Palermo, Italy

Draft version March 21, 2018

ABSTRACT

Magnetic reconnection plays an integral part in nearly all models of solar flares and coronal mass ejections (CMEs). The reconnection heats and accelerates the plasma, produces energetic electrons and ions, and changes the magnetic topology to form magnetic flux ropes and allow CMEs to escape. Structures that appear between flare loops and CME cores in optical, UV, EUV and X-ray observations have been identified as current sheets and interpreted in terms of the nature of the reconnection process and the energetics of the events. Many of these studies have used UV spectral observations of high temperature emission features in the [Fe XVIII] and Si XII lines. In this paper we discuss several surprising cases in which the [Fe XVIII] and Si XII emission peaks are spatially offset from each other. We discuss interpretations based on asymmetric reconnection, on a thin reconnection region within a broader streamer-like structure, and on projection effects. Some events seem to be easily interpreted as projection of a sheet that is extended along the line of sight that is viewed an angle, but a physical interpretation in terms of asymmetric reconnection is also plausible. Other events favor an interpretation as a thin current sheet embedded in a streamer-like structure.

Subject headings: Sun: corona, flares, coronal mass ejections, UV radiation

1. INTRODUCTION

Most large solar eruptions involve both an X-ray flare and a coronal mass ejection. While different magnetic topologies and trigger mechanisms are invoked in different scenarios, essentially all of the models include a current sheet where magnetic field rapidly reconnects. The reconnection converts magnetic free energy into heat, kinetic energy and energetic particles to power the flare, and it changes the magnetic topology, which helps the CME to escape. The reconnection also produces a twisted topology, either wrapping more helical field around an existing flux rope (Lin & Forbes 2000; Lin et al. 2004) or creating a flux rope from scratch (Gosling et al. 1995).

A common feature of all flare models is that while magnetic reconnection must be slow under normal circumstances to allow magnetic free energy to build up in the corona before the eruption, fast reconnection is required to match the rapid rise of flare emission during the eruption. In most models reconnection must occur over large area to account for the total energy. On small scales, kinetic effects and the tearing mode instability are crucial (Loureiro et al. 2012; Ji & Daughton 2011; Shen et al. 2013a), while on larger scales the current sheet is described either as a small diffusion region at an X-line with larger scale shock-like structures enclosing an exhaust region (Petschek model) or as a thick turbulent current sheet (Lazarian & Vishniac 1999; Kowal et al. 2009).

Various observations of flares and CMEs have been in-

terpreted in terms of current sheets and used to estimate such parameters as the temperature, thickness, density, turbulent velocity and reconnection rate. The Ultraviolet Coronagraph Spectrometer (UVCS) (Kohl et al. 1995, 1997) observed the high temperature emission line of [Fe XVIII] in narrow features between the post-flare loops and CME cores (Ciaravella et al. 2002; Ko et al. 2003; Bemporad et al. 2006; Ciaravella & Raymond 2008; Schettino et al. 2010), and even higher temperature lines were observed with Solar Ultraviolet Measurements of Emitted Radiation (SUMER) experiment (Innes et al. 2003a,b) and the Interface Region Imaging Spectrograph (IRIS) (Tian et al. 2014). Narrow band EUV images from Extreme-Ultraviolet Imaging Telescope (EIT) and TRACE (Yokoyama et al. 2001; McKenzie 2000) and the Atmospheric Imaging Assembly (AIA) (Reeves & Golub 2011; Savage et al. 2012) have been interpreted in terms of inflow, outflow and heating in the reconnection region. White light features that resemble rays topped by disconnection regions seen in the wakes of some CMEs seem to be current sheets in many cases (Webb et al. 2003; Ciaravella et al. 2013), and hard X-ray emission seems to show hot regions on either side of an X-line in some RHESSI observations (Sui & Holman 2003; Susino et al. 2013).

In the course of comparing white light and UVCS observations of candidate current sheets, Ciaravella et al. (2013) compiled a list of events detected in [Fe XVIII] by UVCS. The [Fe XVIII] λ 975 line emission peaks at $\log T=6.85$ according to version 7 of CHIANTI (Landi et al. 2013), and it is rarely seen with UVCS ex-

cept in CMEs and current sheets. Several of the events in Ciaravella et al. (2013) showed a significant offset between the peak spatial positions of [Fe XVIII] and Si XII $\lambda\lambda 499, 521$. In this paper we quantify those offsets and discuss interpretations in terms of actual physical offsets due to asymmetric reconnection or of projection effects resulting from viewing geometry. Projection effects are a possible explanation for the events with a simple offset, but are less likely to account for events where the [Fe XVIII] emission is centered within a wider Si XII feature. The observations are described in Section 2, while the analysis and results in Section 3. In Section 4 we present the interpretation of the CS characteristics. The discussion and conclusions are in Section 5.

2. OBSERVATIONS

We examined the events from the Ciaravella et al. (2013) list of 28 current sheets detected in the [Fe XVIII] line with UVCS. We excluded events not detected in Si XII and events in which there were too few counts in the [Fe XVIII] line to obtain a good intensity profile along the UVCS slit. The remaining 14 events are listed in Table 1, and details of several individual events are discussed in the Appendix. The number of events is modest because the [Fe XVIII] line was only observable in a small range of grating positions, and the UVCS instrument configuration only covered that wavelength for a small fraction of the time that UVCS was observing. However, almost all UVCS observations covered the O VI doublet, at least one member of the Si XII doublet, and either Ly α or Ly β . The emissivities of these lines peak at different temperatures; $\log T = 6.30$ for Si XII and $\log T = 5.50$ for O VI, but both have significant emissivity at higher temperatures. The Lyman line emission drops off approximately as $T^{-0.5}$, but it also depends on the outflow speed and temperature of the plasma through Doppler dimming.

The UVCS instrument measures the intensities and line profiles of coronal emission lines along a 42' slit which is perpendicular to the radial vector from Sun center to a reference point near the middle of the slit. The slit could be placed at any heliocentric height, but because the intensity drops off rapidly with distance above the surface and we are studying faint lines, all the observations reported here were at 1.91 R_{\odot} from Sun center or lower. The spatial resolution was generally limited by onboard binning mandated by the telemetry rate, and it ranges from 21'' to 70'' for the observations presented here. Many different observing sequences were employed during the life of the mission, so the exposure times vary from a few minutes to a few hours. More details about the observations are given in Ciaravella et al. (2013) and Giordano et al. (2013).

To investigate the spatial relationships among the emission at different temperatures, we measured the intensity profiles of the different spectral lines along the slit. We measured the intensities in two ways in order to assess uncertainties in background subtraction: First, we simply added up the counts above background in each spatial bin, and second, we fit a Gaussian to the profile in each spatial bin. The results for the two measurements are nearly indistinguishable except in cases where there are too few counts for a meaningful Gaussian fit, and in those cases the intensities from adding up the counts

were too noisy to produce significant correlations among the line intensities.

For each event (and for each slit position if more than one were obtained) we performed a cross correlation between the spatial profiles of [Fe XVIII] and the Si XII, O VI and Lyman lines in order to quantify the separations between features seen at different temperatures in an objective manner. The spatial morphology of [Fe XVIII] intensity is a single or double peak. In the latter cases the correlation analysis has been performed for each peak separately. The results will be discussed in more detail in section 3.

3. ANALYSIS AND RESULTS

The results of our cross correlation analysis are in Table 1. For each event we list the data and time of the observation, the height, Position Angle, the spatial width of the [Fe XVIII] line and, the cross correlation parameters (factor, lag and width) with Si XII, O VI and Ly β (α) lines. Here, the lag is the spatial separation between the peaks seen in different lines. The spatial width has been computed as the FWHM of the [Fe XVIII] intensity distribution along the UVCS slit. In the last column of Table 1, we also give a classification based on the spatial profiles of [Fe XVIII] and Si XII; "S" if the profiles are basically the same, "O" if they are similar but offset from each other, and "I" if the [Fe XVIII] emission lies within a broader Si XII feature. The 3 events marked with 'b' in Table 1 are those in which [Fe XVIII] spatial profiles show two peaks. Generally the two peaks do not appear in the UV spectra simultaneously. In some cases one peak appears during the observation as associated to a CME. In other cases the peaks are detected since the beginning of the observation, and they may or may not be easily associated with a CME observed in WL. The two peaks are often different in intensity and spatial distribution. We analyse them separately and in Table 1 we present the results for the peak that has been associated with a CME in WL.

We initially took 0.8 as the threshold for a meaningful cross correlation coefficient, but in several cases and unrelated emission far from the CS reduced the correlation coefficient in spite of a close relationship in the vicinity of the CS. Therefore, we relax the threshold to 0.7 and list the coefficients, lags and widths in Table 1. We note that in quite a few cases, the Ly α and O VI peaks are very broad and are probably unrelated foreground or background emission, but in some cases there is a narrow peak of emission related to the current sheet as well. Figures 1 through 4 present examples of 1) an event with [Fe XVIII] and Si XII essentially coincident, 2) an event with strong [Fe XVIII] and Si XII peaks offset from each other, 3) an event with no meaningful correlation between [Fe XVIII] and the other lines, and 4) an event with [Fe XVIII] and Si XII peaking at the same place, but with Si XII spatially wider than [Fe XVIII].

4. INTERPRETATION

4.1. Observational signatures of physical structure

In the simplest picture of a current sheet, the one evoked by 2D cartoons of solar eruptions, cool material flows symmetrically into the CS from the sides, is strongly heated and flows out the top and bottom of the CS. Because dissipation of magnetic flux decreases the

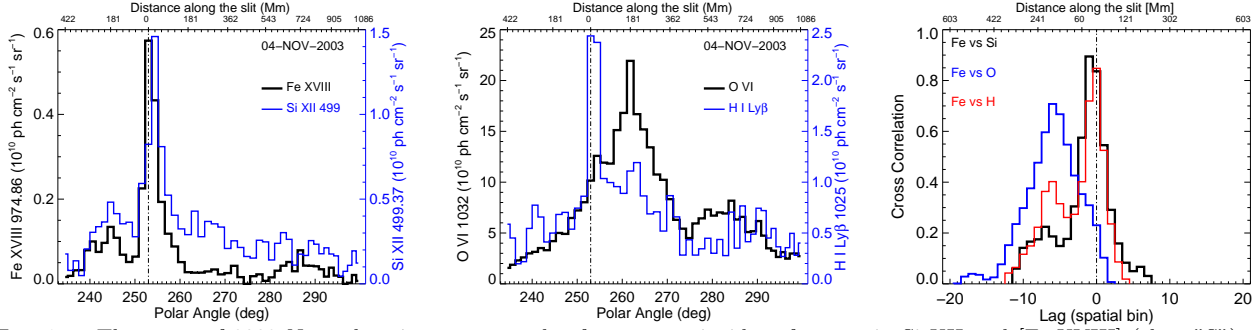


FIG. 1.— The event of 2003 November 4 as an example of narrow, coincident features in Si XII and [Fe XVIII] (class “S”). The left panel shows the intensities of the [Fe XVIII] and Si XII lines (with the Si XII scale on the right) as functions of position along the slit with UVCS mirror pointed to $1.67 R_{\odot}$. The vertical dashed line indicates the peak of the [Fe XVIII] intensity. In the middle panel are the O VI $\lambda 1032$ and Ly β lines. The right panel shows the cross correlations between [Fe XVIII] and Si XII (black), O VI (blue) and Ly α (red).

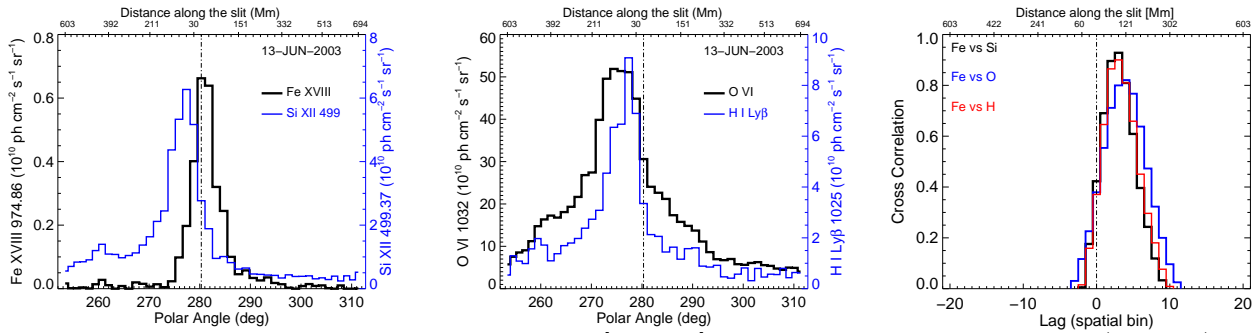


FIG. 2.— The event of 2003 June 13 as an example of sharp [Fe XVIII] and Si XII that are significantly offset (class “O”). The panels present data as in Figure 1. UVCS mirror is pointed to $1.67 R_{\odot}$.

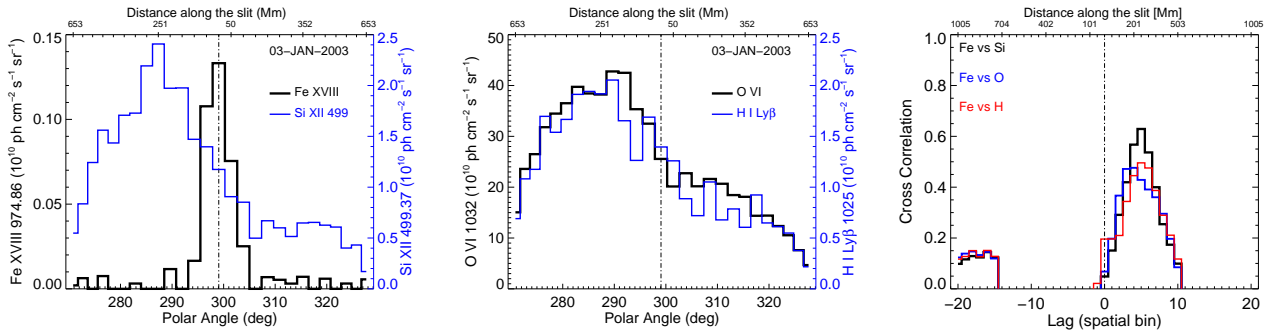


FIG. 3.— The event of 2003 January 03 as an example of an event with no feature in Si XII that is correlated with the [Fe XVIII] feature (class “O”). The panels present data as in Figure 1. UVCS mirror is pointed to $1.72 R_{\odot}$.

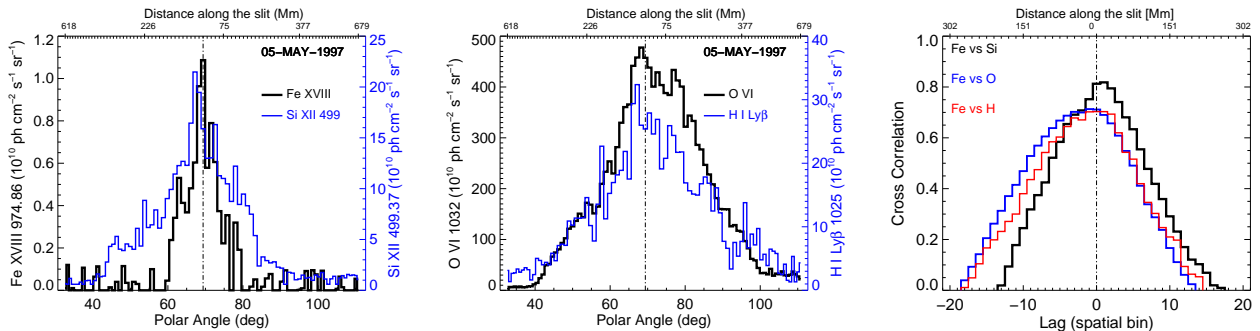


FIG. 4.— The event of 1997 May 05 as an example of an [Fe XVIII] feature within a broader Si XII emission feature (class “I”). The panels present data as in Figure 1. UVCS mirror is pointed to $1.14 R_{\odot}$.

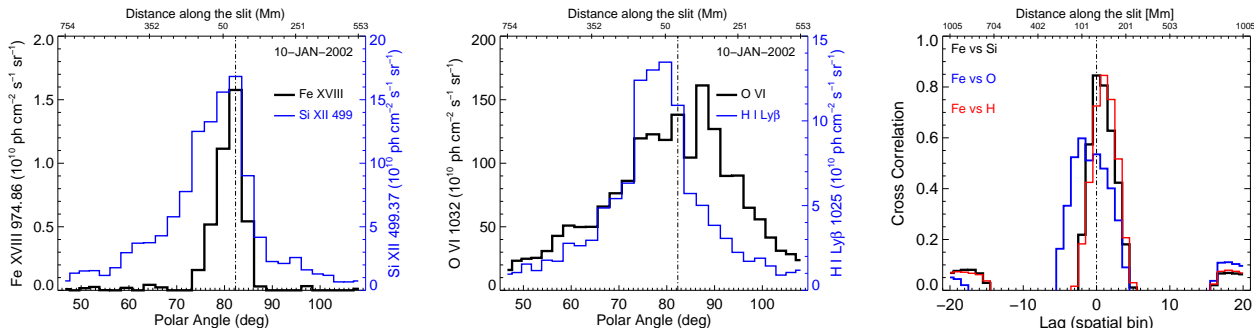


FIG. 5.— The event of 2002 January 10 as another example of an [Fe XVIII] feature within a broader Si XII emission feature (class "P"). The panels present data as in Figure 1. UVCS mirror is pointed to $1.57 R_{\odot}$. In this case the [Fe XVIII] and Si XII peaks occur in the same place, but the [Fe XVIII] peak is symmetric and the Si XII peak is not.

magnetic pressure, the density increases in the current sheet if the plasma β is low. Thus one expects a thin sheet of [Fe XVIII] and Si XII emission due to the high temperature and increased density in the current sheet. (For the purposes of this paper, "thin" means that the thickness is small compared to the scale of the CME, but the CS can still be orders of magnitude thicker than the classical CS thickness of the Sweet-Parker mechanism.) There may also be a gap of the emission in the cooler lines, though a gap will only appear if the current sheet occupies a substantial fraction of the line of sight within a spatial bin. The reduced ionization fractions of O VI and H I at the higher temperatures would be at least partly compensated by the higher density, but Doppler dimming associated with the CS outflow would reduce the emission in O VI and Ly β and severely reduce the Ly α emission (Lin et al. 2005).

Several variations are possible. If the central temperature is well above the formation temperature of [Fe XVIII], there could be two sheets of [Fe XVIII] separated by region that would be dim in all the lines. One possible example will be discussed below. Consideration of time-dependent ionization (Ko et al. 2010; Shen et al. 2013b) could alter the emission patterns in the CS, since the ionization state lags behind the jump in the electron temperature. The time-dependent ionization could mean that the inflowing gas is compressed and heated, emits in the lower ionization lines, and gradually ionizes toward [Fe XVIII], giving a thin [Fe XVIII] layer sandwiched between Si XII sheets which in turn lie between O VI sheets. A thermal conduction halo around the current sheet (Imada et al. 2011) could have somewhat similar effects.

In this simple picture, which should apply to either Petschek or turbulent (Lazarian & Vishniac 1999) reconnection, the inflow speed is of order $0.05 V_A$ and the outflow speed is of order V_A according to both observations (Lin et al. 2005; Yokoyama et al. 2001) and theory (Liu et al. 2017). The high temperature emission seen by UVCS often lasts for a long time and persists as the flare X-ray emission subsides (Bemporad et al. 2006; Susino et al. 2013), but it may require only a low level of reconnection relatively high (1.5 to $2 R_{\odot}$) in the corona. At very late times the structure might tend toward that of an ordinary helmet streamer, with a thin current sheet having a slow reconnection rate and slow solar wind flows on both sides, as in the description of the heliospheric current sheet by Wang et al. (2000).

However, in cases with narrow, well-defined emission

features we sometimes see an [Fe XVIII] feature offset along the UVCS slit from a narrow Si XII feature by 30 to 250 Mm. There are several interesting possible explanations for this asymmetry. There is also, of course, the possibility that the [Fe XVIII] and Si XII features are unrelated, which is plausible if the features are very broad and poorly correlated, but not if both are narrow and much brighter than usually seen at that height in the corona. Since there are several of the latter cases, we must consider physical explanations.

1) The reconnection may be asymmetric in the sense that the density or magnetic field is higher on one side than the other. This situation has been explored by Cassak & Shay (2007), Murphy et al. (2012) and Murphy & Lukin (2015). If the plasma β is fairly low, the pre-eruption magnetic field strength is comparable on the two sides, so the Alfvén speed is higher on the low density side. The maximum temperature increase (if heating dominates over bulk kinetic energy and non-thermal particles) is given by energy available to heat the plasma,

$$\Delta T = \frac{2}{3} \frac{B^2}{8\pi n k_B} = \frac{1}{3} \frac{\mu}{k_B} V_A^2 \quad (1)$$

where B is the reconnecting magnetic field corresponding to the magnetic free energy, n is the total particle density, k_B is the Boltzmann constant and μ is the mean particle mass. Here V_A is the Alfvén speed corresponding to the reconnecting field, so the Alfvén speed including the guide field may be higher. Thus the density should be smaller in the higher temperature [Fe XVIII] side than in the Si XII side by roughly the ratio of temperatures, or typically a factor of 1.5 to 2 for modest (factor of 2) density contrasts across the current sheet. The relative brightnesses of the Si XII and [Fe XVIII] lines depend on the densities, the ionization states and on the sizes of the high and low density regions. This simple description assumes that all the dissipated magnetic energy on the two sides goes into heat, while in fact significant fractions may go bulk kinetic energy and non-thermal particles.

2) In the picture where the reconnecting current sheet is located within a structure like a helmet streamer, the Si XII could come from the region outside the current sheet, and there is no reason that the regions on the two sides should be the same. The densities, temperatures, flow speeds and thicknesses of the Si XII layers could be very different, in which case the center of the Si XII emission will be offset from that of the [Fe XVIII] in the CS.

3) A thermal conduction halo, in which some of the heat of electrons within the current sheet warms the inflowing gas outside the CS, appeared in the numerical simulations of Imada et al. (2011). For a Petschek exhaust flow, this requires that thermal conduction carry the energy across the shocks that bound the exhaust. The electric fields in the shocks should inhibit this transport of energy by electrons, so existing models might overestimate the heating.

4.2. Projection effects

The above interpretations apply to a perfectly edge-on viewing angle, but in general the line of sight does not lie exactly along the CS, and the CS is not exactly planar. Projection effects can explain some observed morphologies, though in other cases that explanation seems strained. One of the most interesting results from the UVCS observations of current sheets is the apparent thickness of order tens of Mm, since the Sweet-Parker model predicts thicknesses orders of magnitude smaller. The thicknesses are compatible with the predictions of either turbulent reconnection (Lazarian & Vishniac 1999) or the exhaust regions of Petschek reconnection (Vršnak et al. 2009), though the observed non-thermal line broadening favors the former (Bemporad 2008; Ciaravella & Raymond 2008). However, the observed thickness is just an upper limit if the CS is extended along the LOS direction and the viewing angle differs from edge-on. The actual thickness can be separated from projection effects if another constraint is available. In the best-studied case, that of 2003 November 4, a white light observation from MLSO provides the electron column density, N_e , and UVCS provides the emission measure, EM. Since N_e is the electron density times the depth along the line of sight, and EM is density squared time depth along the line of sight, one can divide one into the other to determine both the density and the thickness of the current sheet (Ciaravella & Raymond 2008).

In regards to offsets between Si XII and [Fe XVIII] emission, consider a current sheet near the solar limb that is extended along the line of sight and whose temperature decreases from the near end to the far end. In that case, Si XII will be brighter near the far end, and [Fe XVIII] will be brighter at the near end. If the sheet is edge-on, the intensity peaks will coincide, and the [Fe XVIII] to Si XII ratio will give an average temperature. However, if the CS is tilted with respect to the LOS, the [Fe XVIII] and Si XII will appear to be offset. In the simple case of a linear change in temperature, the [Fe XVIII] to Si XII ratio and the temperature derived from that ratio will appear to change continuously along the slit. In the case of the 2003 June 13 observation shown in Figure 2, a temperature changing from 2.5×10^6 to 5×10^6 K across the Si and Fe features could account for the observations. However, there is likely to be some foreground or background Si XII emission, and temperatures away from the peaks are not reliable.

There are two kinds of morphology that are difficult to explain with projection. In a case where the CS appears as a deficit in low temperature emission lines, a thin current sheet seen at an angle could produce only a very slight reduction of the brightness. This situation was reported by Lin et al. (2005). The second case is one

where the [Fe XVIII] is located inside a broader Si XII feature, as is seen in Figure 4. In principle, there could be a wavy sheet with temperature variations such that the hottest portions happen to lie at the projected center, while the cooler portions are off to the sides, but such a geometry is very contrived. A CS extended along the LOS with a temperature peaking in the middle is possible, but somewhat ad hoc.

Overall, projection effects can potentially explain simple offsets between Si XII and [Fe XVIII] peaks if the CS is sufficiently extended along the LOS, hotter at one end than the other, and seen at a modest inclination. It is difficult to distinguish between this explanation and physical explanations such as asymmetric reconnection or a current sheet embedded in an asymmetric helmet streamer structure. Stereoscopic observations might determine which explanation is correct. Estimates of the length and orientation of the CS based on the magnetic configuration before the eruption (for instance Lee et al. (2009)) could offer some less direct constraints.

5. DISCUSSION AND SUMMARY

Magnetic reconnection in current sheets is an integral part of theoretical models of solar flares and CMEs. Structures observed in the UV have been interpreted as examples of these current sheets and used to investigate properties of the reconnection. Some of these structures show a surprising offset between the features seen in Si XII emission lines and the [Fe XVIII] line formed at a temperature 2 to 3 times higher, with offsets of 30 to 180 Mm in several events.

The classification in Table 1 is somewhat subjective, but we see 6 events in which the structures seen in Si XII and [Fe XVIII] are basically the same, suggesting a simple structure with a constant temperature or range of temperatures. It is also possible that these events have current sheets with different temperatures at the front and back ends, but that the CS is very closely aligned with the line of sight. How close this alignment must be depends on the length of the CS, which is not known except in the case of the 2003-11-04 event, where the actual thickness and LOS length were comparable and the uncertainty in the offset precludes an accurate determination of the angle or a reliable limit on the temperature change along the CS.

Table 1 also shows 4 offset ("O") events. The number of "O" events is similar to the number of "S" events with similar Si XII and [Fe XVIII] structures. That would be consistent with line-of-sight depths comparable to the apparent thicknesses and a random distribution of viewing angles. Given the small number of events, projection of a CS seen not quite edge-on seems capable of explaining the observations, though the symmetric [Fe XVIII] peaks in well resolved events such as 2003-06-13 (Fig. 2) would then be a coincidence. The observations could also be explained by asymmetric reconnection, which would require that the cooler and hotter sides of the CS remain separate. That question has not been addressed for turbulent CS, and it would seem problematic in the classical Petschek picture, but a guide field might maintain the temperature separation.

Four events show an [Fe XVIII] peak lying within a broader Si XII structure. One plausible interpretation is that the Si XII is a helmet streamer, and the [Fe XVIII]

TABLE 1

Event	UT	Height	PA	Fe XVIII ^c	Cross Correlation Parameters			Class
		R _⊙	°	10 ⁶ m	Si XII	(r)(lag - width) × 10 ⁶ m O VI	Lyβ(α)	
97-05-05	17:36	1.14	67	143	(0.8) 15 -211	(0.7) 0 -271	(0.7) 30 - 256	I
98-03-23 ^b	16:00	1.51	235	164	(0.8) 30-181	(0.8) 0-241	(0.7) 120-241	I
98-04-20	17:10	1.20	245	195	(0.9) 0-181	(0.9) 60- 211	(0.9) -30 -181	S
	17:46	1.25	244	202	(0.9) 0-241	(0.9) 60-241	(0.9) 30 - 241	S
	18:01	1.31	244	199	(0.8) 0-241	(0.9) 60-241	(0.8) 30-241	S
	18:39	1.36	245	219	(0.7) 0-271	(0.8) 90-302	(0.7) 120-332	S
	18:50	1.41	245	225	(0.8) 0-332	(0.8) 60-302	(0.8) 30-241	S
	19:36	1.46	244	328	(0.8) 0-302	(0.8) 90-332	(0.8) 30-302	S
00-02-22	18:39	1.45	46	79	(0.7) 151-302	(0.7) 211-332	(0.7) 241-392	O
	18:50	1.51	48	156	(0.7) 180-362	(0.7) 241-332	(0.6) 241-392	O
01-10-31	04:27 ^a	1.53	92	139	(0.8) 166-196	(0.6) 15-377	(0.6) 150-347	O
01-11-02	02:23 ^a	1.52	273	173	(0.7) 0-211	(0.5) 0- 362	(0.6) 0-302	S
01-12-20 ^b	23:20	1.59 ^a	271	125	(0.7) 150-302	(0.5) 301-402	(0.6) 150-302	O
		1.56	281	174	(0.8) 0-302	(0.6) 100-402	(0.8) 0-302	S
01-12-21	09:20	1.91	280	464	(0.9) 150-352	(0.8) 251-402	(0.8) 150-352	S
02-01-10	20:45	1.57	280	116	(0.9) 0-201	(0.6) 100-302	(0.9) 50-201	I
03-01-03	11:35	1.72	299	121	(0.6) 251-201	(0.5) 201-302	(0.5) 251-251	O
03-06-02	06:08	1.73 ^a	250	225	(0.4) 60-814	(0.6) 150-221	(0.7) 90-151	I
03-06-02	10:06	1.69	257	124	(0.7) 30-151	(0.7) 30-181	(0.7) 90-151	I
03-06-13	17:23	1.67	280	113	(0.9) 90-151	(0.8) 121-211	(0.9) 90-151	O
03-11-03 ^b	11:07	1.75	269	180	(0.8) 30-181	(0.7) 120-211	(0.7) 90-181	I
03-11-04	20:30	1.69	253	70	(0.9) 0-90	(0.7) 181-211	(0.8) 0-241	S

^a low statistics

^b double peak

^c spatial size of the current sheet in Mm, evaluated as the FWHM of the Fe XVIII intensity distribution along the UVCS slit.

represents a hot, narrow CS within it. In the case of the 2002-01-10 event (Figure 5), the difference between the Si XII structure and the structures seen in Lyβ and O VI, both of which show a drop where the [Fe XVIII] peaks, suggests that the helmet streamer itself is asymmetric. The intensity drop in the cool lines indicates that the hot CS gas must occupy a substantial fraction of the volume near the [Fe XVIII] peak. We note, however, that in many events the peak seen in [Fe XVIII] and Si XII seems virtually unrelated to the much broader emission in O VI and the Lyman lines, and in these cases the cool emission might arise in foreground or background gas unrelated to the CS.

Only one event, that of 2001-12-20, shows a double peak in [Fe XVIII] that might have a physical origin. The others have a pre-existing peak, sometimes associated with an earlier CME as in the 1998-03-23, 2003-11-03 and 2003-11-04 events, and a new peak appears nearby after a CME. That also might be the explanation for the 2001-12-20 event, since the [Fe XVIII] peak near PA=280° remains constant while the narrow bright peak at PA=271° fades away. However, a physical interpretation in terms of gas hotter than the [Fe XVIII] peak is also possible.

Overall, offsets between the CS structures seen in

[Fe XVIII] and Si XII can have an interesting physical interpretations such as asymmetric reconnection, or the mundane interpretation in terms of projection effects. The currently existing data does not allow us to discriminate among them with certainty, because a configuration can be invented to explain almost any observation with projection effects. However, in some cases (simple offsets) the projection explanation is plausible because it arises from a configuration that is likely to occur, while in other cases (narrow [Fe XVIII] centered in a broad Si XII feature) it would require a much less probable configuration. Further progress could come with higher quality observations that permit study of fine scale structure, temporal variations or more detailed temperature and density determinations. Other avenues for resolving the ambiguity would be stereoscopic viewing or MHD modeling that could predict the morphology of the current sheet. Perhaps a systematic study of CS seen during flares with AIA will reveal the extent of temperature variations along those structures and make the projection hypothesis more or less favored.

This work was partially supported by NASA grants NNH14AX61I and NNX13AG54G and by N00173-14-1-G908 the NASA LWS grant NNH13ZDA001N. SOHO (UVCS).

APPENDIX

APPENDIX MATERIAL

1998-03/23: This event was studied by Ciaravella et al. (2002). There is a narrow, bright [Fe XVIII] peak, which we take to be the CS, and a weaker more diffuse peak to the south, which we take to be a long-lasting, bright active region.

2001-12-20: This event shows a very clear double peak in [Fe XVIII] with a 180 Mm separation during the first 2 hours, which evolves to a narrow peak offset from Si XII and finally a broader peak coincident with Si XII. The Si XII structure is similar to that of Lyβ, and it remains fairly constant.

2002-01-10: This long-lasting CS was studied by Ko et al. (2003). There is a dip in the low temperature emission corresponding to a peak in the high temperature lines, indicating that the CS is extended along the line of sight and that its thickness is comparable to the spatial resolution of the observations.

2003-06-02: Details of this event are shown in Schettino et al. (2010) .

2003-06-13: This event is unusual in that fairly narrow O VI and Ly β show a similar structure to Si XII, somewhat offset from [Fe XVIII].

2003-11-04: This event was studied by Ciaravella & Raymond (2008). For the analysis of this CS we used the data from 22:59/04 to 01:59/05 to exclude several blobs of very cool, very bright emission in the H I, C III and O VI lines about 250-300", or about 180-240 Mm away from the [Fe XVIII] feature. These blobs are probably small, secondary ejections of prominence material that are channeled along field lines close to the CS, probably in a streamer-like structure. The correlated feature in Ly β indicates a high density in the CS.

REFERENCES

- Bemporad, A. 2008, ApJ, 689, 572
 Bemporad, A., Poletto, G., Suess, S. T., et al. 2006, ApJ, 638, 1110
 Cassak, P. A., & Shay, M. A. 2007, Physics of Plasmas, 14, 102114
 Ciaravella, A., Raymond, J. C., Li, J., et al. 2002, ApJ, 575, 1116
 Ciaravella, A. & Raymond, J.C. 2008, ApJ, 686, 1372
 Ciaravella, A., Webb, D.F., Giordano, S. & Raymond, J.C. 2013, ApJ, 766, 65
 Giordano, S., Ciaravella, A., Raymond, J. C., Ko, Y.-K., & Suleiman, R. 2013, Journal of Geophysical Research (Space Physics), 118, 967
 Gosling, J. T., Birn, J., & Hesse, M. 1995, Geophys. Res. Lett., 22, 869
 Imada, S., Murakami, I., Watanabe, T., Hara, H., & Shimizu, T. 2011, ApJ, 742, 70
 Innes, D. E., McKenzie, D. E., & Wang, T. 2003, Sol. Phys., 217, 267
 Innes, D. E., McKenzie, D. E., & Wang, T. 2003, Sol. Phys., 217, 247
 Ji, H., & Daughton, W. 2011, Physics of Plasmas, 18, 111207
 Ko, Y.-K., Raymond, J. C., Lin, J., et al. 2003, ApJ, 594, 1068
 Ko, Y.-K., Raymond, J. C., Vršnak, B., & Vujčić, E. 2010, ApJ, 722, 625
 Kohl, J. L., Esser, R., Gardner, L. D., et al. 1995, Sol. Phys., 162, 313
 Kohl, J. L., Noci, G., Antonucci, E., et al. 1997, Sol. Phys., 175, 613
 Kowal, G., Lazarian, A., Vishniac, E. T., & Otmianowska-Mazur, K. 2009, ApJ, 700, 63
 Landi, E., Young, P. R., Dere, K. P., Del Zanna, G., & Mason, H. E. 2013, ApJ, 763, 86
 Lazarian, A., & Vishniac, E. T. 1999, ApJ, 517, 700
 Lee, J.-Y., Raymond, J. C., Ko, Y.-K., & Kim, K.-S. 2009, ApJ, 692, 1271
 Lin, J., & Forbes, T. G. 2000, J. Geophys. Res., 105, 2375
 Lin, J., Raymond, J. C., & van Ballegoijen, A. A. 2004, ApJ, 602, 422
 Lin, J., Ko, Y.-K., Sui, L., et al. 2005, ApJ, 622, 1251
 Lin, J., Li, J., Ko, Y.-K., & Raymond, J. C. 2009, ApJ, 693, 1666
 Liu, Y.-H., Hesse, M., Guo, F., Daughton, W., Li, H., Cassak, P.A. & Shay, M.A. 2017, PhReL, 118, 5101
 Loureiro, N. F., Samtaney, R., Schekochihin, A. A., & Uzdensky, D. A. 2012, Physics of Plasmas, 19, 042303
 McKenzie, D. E. 2000, Sol. Phys., 195, 381
 Murphy, N. A., Miralles, M. P., Pope, C. L., et al. 2012, ApJ, 751, 56
 Murphy, N. A., & Lukin, V. S. 2015, arXiv:1504.01425
 Raymond, J. C., Ciaravella, A., Dobrzycka, D., et al. 2003, ApJ, 597, 1106
 Reeves, K. K., & Golub, L. 2011, ApJ, 727, L52
 Savage, S. L., Holman, G., Reeves, K. K., et al. 2012, ApJ, 754, 13
 Schettino, G., Poletto, G. & Romoli, M. 2010, ApJ, 708, 1135
 Shen, C., Lin, J., Murphy, N. A., & Raymond, J. C. 2013a, Physics of Plasmas, 20, 072114
 Shen, C., Reeves, K. K., Raymond, J. C., et al. 2013b, ApJ, 773, 110
 Sui, L., & Holman, G. D. 2003, ApJ, 596, L251
 Susino, R., Bemporad, A., & Krucker, S. 2013, ApJ, 777, 93
 Tian, H., Li, G., Reeves, K.K., et al. 2014, ApJ, 797, L14
 Vršnak, B., Poletto, G., Vujčić, E., et al. 2009, A&A, 499, 905
 Wang, Y.-M., Sheeley, N. R., Socker, D. G., Howard, R. A., & Rich, N. B. 2000, J. Geophys. Res., 105, 25133
 Webb, D. F., Burkepile, J., Forbes, T. G., & Riley, P. 2003, Journal of Geophysical Research (Space Physics), 108, 1440
 Yokoyama, T., Akita, K., Morimoto, T., Inoue, K., & Newmark, J. 2001, ApJ, 546, L69